

Preparation, Structure, and Properties of the Arsenic-Containing Corner-Shared Double Cube $[\text{Mo}_6\text{AsS}_8(\text{H}_2\text{O})_{18}]^{8+}$: Metal–Metal Bonding and a Classification of Different Cluster Types

Rita Hernandez-Molina, Andrew J. Edwards, William Clegg, and A. Geoffrey Sykes*

Department of Chemistry, The University of Newcastle, Newcastle upon Tyne, NE1 7RU U.K.

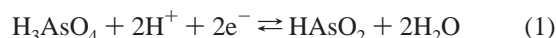
Received December 16, 1997

The trinuclear Mo^{IV}_3 incomplete cuboidal cluster $[\text{Mo}_3\text{S}_4(\text{H}_2\text{O})_9]^{4+}$ in 2 M HCl reacts rapidly (green to intense blue-green color change) with AsO_2^- or HAsO_4^{2-} in the presence of H_3PO_2 as reductant to give the new air-sensitive corner-shared double cube $[\text{Mo}_6\text{AsS}_8(\text{H}_2\text{O})_{18}]^{8+}$. Purification by Dowex 50W-X2 cation-exchange chromatography requires 4 M H(pts) (pts = *p*-toluenesulfonic acid) for elution, consistent with a high charge. The X-ray structure has been determined for crystals obtained from 4 M H(pts) solution, full formula $[\text{Mo}_6\text{AsS}_8(\text{H}_2\text{O})_{18}](\text{pts})_8 \cdot 28\text{H}_2\text{O}$. The Mo_6AsS_8 core structure was confirmed from ICP elemental analysis for Mo, As, and S (6:1:8) and the 8+ charge from the 3:1 stoichiometries with $[\text{Co}(\text{dipic})_2]^-$ and $[\text{Fe}(\text{H}_2\text{O})_6]^{3+}$ as oxidant. Rate constants for the oxidation of $[\text{Mo}_6\text{AsS}_8(\text{H}_2\text{O})_{18}]^{8+}$ with $[\text{Co}(\text{dipic})_2]^-$ have been determined and indicate strong reduction properties as compared to other heteroatom clusters. The existence of short (bonding) Mo–Mo separations, 2.716 Å average, and long (nonbonding) Mo–As separations at 3.554 Å, together with similar features for other heteroatom clusters, has led to a classification of the clusters into different categories. The nine 8+ double cubes, most of which contain a main group heteroatom M, are classified as $(\text{Mo}_3\text{S}_4^{4+})_2\text{M}^0$, with retention of two metal–metal bonded $\text{Mo}_3\text{S}_4^{4+}$ units. The single cubes, on the other hand, can be classified as $\text{Mo}_3\text{S}_4^{4+}\text{M}^0$, with M a transition metal, or $\text{Mo}_3\text{S}_4^{4+}\text{M}^x$, with M a main group element (*x* depends on group involved).

Introduction

Corner-shared double-cube heteroatom (M) derivatives of the cuboidal Mo^{IV}_3 incomplete cuboidal complex $[\text{Mo}_3\text{S}_4(\text{H}_2\text{O})_9]^{4+}$, of general formula $[\text{Mo}_6\text{MS}_8(\text{H}_2\text{O})_{18}]^{8+}$, have been prepared by incorporation of a number of election-rich M (d^{10} or greater) main group elements.^{1–3} These include Sb, Bi (group 15),^{4,5} Sn, Pb (group 14),^{6–8} In, Tl (group 13),^{9–11} and Hg (group 12).¹² Here we explore the incorporation of As (group 15), an element which, in terms of electronegativity, is at the border of nonmetallic and metalloid behavior, into $[\text{Mo}_3\text{S}_4(\text{H}_2\text{O})_9]^{4+}$. Whereas cationic forms of Sb^{III} and Bi^{III} occur in aqueous solution and $[\text{Bi}(\text{H}_2\text{O})_9]^{3+}$, for example, is well characterized,¹³

As^{III} is present in acidic solutions as $\text{As}(\text{OH})_3$ or related forms. The reduction potential for the $\text{As}^{\text{V}}/\text{As}^{\text{III}}$ couple in acidic solutions



($\text{p}K_{\text{a}}$ for $\text{H}_3\text{AsO}_4 = 2.3$) is 0.560 V,¹⁴ and As^{V} is the more stable form in aerated aqueous solutions. Cullen and Reimer¹⁵ have reviewed the aqueous chemistry of As, and other recent reviews on As have appeared.^{16,17} The quite extensive chemistry of arsenic sulfides and related compounds has been summarized.¹⁸

Experimental Section

Preparation of $[\text{Mo}_3\text{S}_4(\text{H}_2\text{O})_9]^{4+}$. Stock solutions of the green Mo^{IV}_3 incomplete cube $[\text{Mo}_3\text{S}_4(\text{H}_2\text{O})_9]^{4+}$ in 2 M HCl were prepared from the Mo^{V}_2 complex $[\text{Mo}_2\text{O}_2(\mu\text{-S})_2(\text{Cys})_2]^{2-}$ (Cys = cysteine)¹⁹ or from polymeric $\{\text{Mo}_3\text{S}_7\text{Br}_4\}_x$ as previously described.²⁰ Details of the UV–vis spectrum are given below.

Other Reagents. Acids used were concentrated HCl (Aldrich), HClO_4 (70%, Fisons), and crystalline *p*-toluenesulfonic acid (Aldrich). Crystalline Li(pts) was prepared by adding stoichiometric amounts of Li_2CO_3 to a solution of H(pts) (4 M) and recrystallizing twice. A sample of $\text{NH}_4[\text{Co}(\text{dipic})_2]\cdot\text{H}_2\text{O}$, (dipic = 2,6-dicarboxylatopyridine),

- (1) Shibahara T, *Adv. Inorg. Chem.* **1991**, 37, 143–173.
- (2) Sellsell, D. M.; Sokolov, M. N.; Sykes, A. G. In *Transition Metal Sulfur Chemistry*; Stiefel, E. I., Matsumoto, K., Eds.; ACS Symposium Series 653; American Chemical Society: Washington, DC, 1996; pp 216–224.
- (3) Sellsell, D. M.; Sykes, A. G. *J. Cluster Sci.* **1995**, 6, 449–461.
- (4) Shibahara, T.; Hashimoto, K.; Sakane, G. *J. Inorg. Biochem.* **1991**, 43, 280.
- (5) Sellsell, D. M.; Sykes, A. G. *Inorg. Chem.* **1996**, 35, 5536.
- (6) Akashi, H.; Shibahara, T. *Inorg. Chem.* **1989**, 28, 2906.
- (7) Varey, J. E.; Lamprecht, G. J.; Fedin, V. P.; Holder, A.; Clegg, W.; Elsegood, M. R. J.; Sykes, A. G. *Inorg. Chem.* **1996**, 35, 5525.
- (8) (a) Sellsell, D. M.; Huang, Z.-X.; Sykes, A. G. *J. Chem. Soc., Dalton Trans.* **1996**, 2623. (b) Sellsell, D. M.; Sykes, A. G. *Inorg. Chem.* **1997**, 36, 2700.
- (9) Sakane, G.; Yao, Y.-G.; Shibahara, T. *Inorg. Chim. Acta* **1994**, 216, 13.
- (10) Hernandez-Molina R.; Fedin V. P.; Sokolov, M. N.; Sellsell D. M.; Sykes, A. G., manuscript in preparation.
- (11) Varey, J. E.; Sykes, A. G. *Polyhedron* **1996**, 15, 1887.
- (12) Shibahara, T.; Akashi, H.; Yamasaki, M.; Hashimoto, K. *Chem. Lett.* **1991**, 689.
- (13) Frank, W.; Reiss, G. J.; Schneider, J. *Angew. Chem., Int. Ed. Engl.* **1995**, 34, 2416.

- (14) Cotton, F. A.; Wilkinson, G. *Advances in Inorganic Chemistry* 5th ed.; Wiley Science: 1988; p 430.
- (15) Cullen, W. R.; Reimer, K. J. *Chem. Rev.* **1989**, 89, 713.
- (16) Francesconi, K. A.; Edmonds, J. S. *Adv. Inorg. Chem.* **1996**, 44, 147–189.
- (17) Dixon, H. B. F. *Adv. Inorg. Chem.* **1996**, 44, 191–227.
- (18) Greenwood, N. N.; Earnshaw, A. *Chemistry of the Elements*, 2nd ed.; Butterworth-Heinemann, Oxford, UK, 1997; pp 518–581.
- (19) Martinez, M.; Ooi, B.-L.; Sykes, A. G. *J. Am. Chem. Soc.* **1987**, 109, 4615.
- (20) Sokolov, M. N.; Coichev, N.; Moya, H. D.; Hernandez-Molina, R.; Borman, C. D.; Sykes, A. G., *J. Chem. Soc. Dalton Trans.* **1997**, 1863.

Table 1. Crystallographic Data

formula	C ₃₆ H ₁₄₈ AsMo ₆ O ₇₀ S ₁₆	fw	3105.3
<i>a</i> , Å	13.5636(8)	space group	<i>P</i> 1
<i>b</i> , Å	14.0548(8)	temp, °C	-113
<i>c</i> , Å	18.4060(10)	<i>λ</i> , Å	0.710 73
<i>α</i> , deg	92.932(2)	<i>V</i> , Å ³	2933.8(3)
<i>β</i> , deg	104.776(2)	<i>D</i> (calc), g cm ⁻³	1.758
<i>γ</i> , deg	118.038(2)	<i>μ</i> , cm ⁻¹	12.9
<i>R</i> ^a	0.0710	<i>Z</i>	1
<i>R</i> _w ^a	0.1590		

^a Conventional $R = \sum(|F_o| - |F_c|)/\sum|F_o|$ for reflections with $F_o^2 > 2\sigma(F_o^2)$; $R_w = \{\sum[w(F_o^2 - F_c^2)^2]/\sum[w(F_o^2)^2]\}^{1/2}$ for all data.

peak 510 nm ($\epsilon = 630 \text{ M}^{-1}\text{cm}^{-1}$), was prepared as previously.⁷ To obtain $[\text{Fe}(\text{H}_2\text{O})_6]^{3+}$, a solution of the perchlorate salt (Fluka) was loaded onto a Dowex column, washed with 0.2 M H(pts), and eluted ($\sim 0.08 \text{ M}$) with 1 M H(pts). Sodium arsenite (NaAsO₂, BDH), sodium hydrogen arsenate (Na₂HAsO₄·7H₂O, Aldrich), and hypophosphorous acid (50% w/w H₂O solution, Aldrich) were used. [CAUTION: All procedures using As-containing compounds and H₃PO₂ as reductant were carried out in a fumehood since AsH₃ may form].

X-ray Crystallography. Principal crystallographic data are given in Table 1. A thin plate crystal of size $0.40 \times 0.20 \times 0.01 \text{ mm}^3$, encapsulated in a film of inert oil, was examined on a Siemens SMART CCD area detector diffractometer. Cell parameters were refined from the observed setting angles of all strong reflections in the complete data set, which was measured by narrow-slice ω scans covering well over a hemisphere of reciprocal space.²¹ Absorption corrections²² were based on multiple and symmetry-equivalent reflections in the data set. A total 21 927 measured data yielded 13 411 unique reflections with $2\theta < 58^\circ$, $R_{\text{int}} = 0.0362$, and maximum indices 17,18,24; 10 560 reflections had $F_o^2 > 2\sigma(F_o^2)$.

The structure was solved by direct methods and refined by full-matrix least-squares²³ on all F^2 values, with weighting $w^{-1} = \sigma^2(F_o^2) + (0.0583P)^2 + (12.7073P)$, where $P = (F_o^2 + 2F_c^2 + F_c^2)/3$. For each of the pts⁻ anions, 2-fold disorder of orientation for the aromatic ring was resolved and refined, the two components being of approximately equal occupancy in each case. Some of the water molecules of crystallization were also disordered. Refinement of disorder was aided by restraints on geometry and displacement parameters, which were anisotropic for all non-H atoms. Hydrogen atoms were included for pts⁻ anions with a riding model, but no H atoms were included for H₂O ligands or molecules. The As atom was constrained to lie on an inversion center.

The goodness of fit was 1.112 for all data and 875 refined parameters. Residual electron density peaks, up to 1.57 e \AA^{-3} , were found close to disordered water molecules, indicating imperfect modeling of the disorder.

Spectrophotometric Studies. Stoichiometry and other measurements were done by standard UV-vis spectrophotometry on a Perkin-Elmer Lambda 9 at $25.0 \pm 0.1^\circ \text{C}$ using H(pts) solutions of $[\text{Mo}_6\text{AsS}_8(\text{H}_2\text{O})_{18}]^{8+}$, ionic strength adjusted to $I = 2.00 \pm 0.01 \text{ M}$ with Li(pts). Kinetic runs were with the oxidant in large, >30 -fold excess. All such runs were carried out on an Applied Photophysics stopped-flow spectrophotometer, and absorbance/time traces were fitted using kinetic software programs provided.

Results

Preparation of $[\text{Mo}_6\text{AsS}_8(\text{H}_2\text{O})_{18}]^{8+}$. A solution of $[\text{Mo}_3\text{S}_4(\text{H}_2\text{O})_9]^{4+}$ (25 mL, 3 mM) in 0.5 M HCl was deoxygenated by bubbling N₂ through for 30 min and then siphoned into a similarly deoxygenated conical flask containing sodium arsenite (0.2 g). Hypophosphorous acid (H₃PO₂, 1 mL of 50% w/w

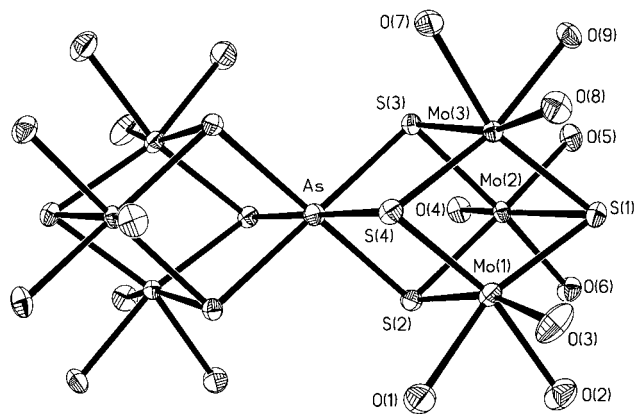
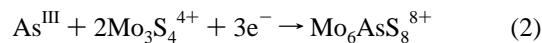


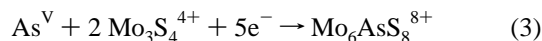
Figure 1. View of the corner-shared double cube $[\text{Mo}_6\text{AsS}_8(\text{H}_2\text{O})_{18}]^{8+}$, with 50% probability ellipsoids and labeling of unique atoms.

H₂O solution) was added as reductant. A rapid color change to a more intense blue-green was observed. After 1 h, the solution was loaded onto a Dowex 50W-X2 cation-exchange column. Rigorous air-free conditions were maintained throughout, and a double-walled column kept at 0°C by circulating ice-cooled water was used. If the solution is allowed to stand for longer periods, i.e., 1 day before loading, a black precipitate forms and decomposition is evident. The column was washed with 0.5 M HCl and then 1 M HCl (both 100 mL). No unreacted $[\text{Mo}_3\text{S}_4(\text{H}_2\text{O})_9]^{4+}$ was eluted at this stage, indicating 100% conversion to product. The latter was eluted with 2 M HCl. A black-brown precipitate remains at the top of the column. The reaction is summarized by (2).



The cluster can, alternatively, be washed with H(pts) solutions and eluted with 4 M H(pts). It is not eluted with 2 M H(pts) (or 4 M HClO₄), consistent with the high 8+ charge in (2). In H(pts), the color is a darker blue.

It is also possible to use sodium hydrogen arsenate as starting material.



No reaction of a single piece of arsenic with $[\text{Mo}_3\text{S}_4(\text{H}_2\text{O})_9]^{4+}$ was observed over 2 weeks or on heating to $70\text{--}80^\circ \text{C}$ for 2 h.

To obtain crystals of a salt of $[\text{Mo}_6\text{AsS}_8(\text{H}_2\text{O})_{18}]^{8+}$, a solution was loaded onto a short Dowex column (6 cm \times 1.5 cm diameter) until saturated, and, after washing, elution was carried out with 4.0 M H(pts). Needle-shaped crystals were obtained after ~ 5 days at $\sim 4^\circ \text{C}$. The crystals have a formula $[\text{Mo}_6\text{AsS}_8(\text{H}_2\text{O})_{18}](\text{pts})_8 \cdot 28\text{H}_2\text{O}$.

Analyses by ICP (atomic emission spectrometry) on a solution in 2 M HCl, purified twice by Dowex column chromatography, gave a Mo:As:S ratio of 5.9:1.0:8.6 (technique less sensitive for S), consistent with $\text{Mo}_6\text{AsS}_8^{8+}$ as the core structure.

X-ray Crystal Structure. The structure of the $[\text{Mo}_6\text{AsS}_8(\text{H}_2\text{O})_{18}]^{8+}$ double-cube cation is shown in Figure 1, with selected bond lengths and angles in Table 2. The As atom lies on a crystallographic inversion center and is octahedrally coordinated by six sulfides. This coordination is trigonally extended, the three S-As-S angles within each cube being significantly below 90° and those between the cubes being correspondingly above. Ignoring Mo-Mo interactions, each Mo is also octahedrally coordinated by three sulfides and three aqua ligands in a *fac* arrangement. The O-Mo-O angles are markedly below 90° , and angular distortions for S-Mo-S are

(21) SMART and SAINT software for area detectors, Siemens Analytical X-ray Instruments, Madison, WI, 1994.

(22) Sheldrick, G. M., SADABS, program for scaling and correction of area detector data, University of Göttingen, Germany, 1997.

(23) Sheldrick, G. M., SHELXTL user manual, Siemens Analytical X-ray Instruments, Madison, WI., Version 5, 1994.

Table 2. Selected Bond Lengths (Å) and Angles (deg)

As(1)–S(2)	2.4454(14)	As(1)–S(3)	2.4890(14)
As(1)–S(4)	2.4338(15)	Mo(1)–S(1)	2.3393(16)
Mo(1)–S(2)	2.3353(16)	Mo(1)–S(4)	2.3391(15)
Mo(1)–S(1)	2.3416(15)	Mo(2)–S(2)	2.3357(15)
Mo(1)–S(3)	2.3397(15)	Mo(3)–S(1)	2.3418(15)
Mo(3)–S(3)	2.3435(15)	Mo(3)–S(4)	2.3405(15)
Mo(1)–O(1)	2.181(5)	Mo(1)–O(2)	2.175(5)
Mo(1)–O(3)	2.154(5)	Mo(2)–O(4)	2.190(4)
Mo(2)–O(5)	2.158(4)	Mo(2)–O(6)	2.149(4)
Mo(3)–O(7)	2.172(4)	Mo(3)–O(8)	2.181(4)
Mo(3)–O(9)	2.157(4)	Mo(1)–Mo(2)	2.7114(7)
Mo(1)–Mo(3)	2.7500(7)	Mo(2)–Mo(3)	2.6878(7)
S(2)–As(1)–S(3)	80.65(5)	S(2)–As(1)–S(4)	82.84(5)
S(3)–As(1)–S(4)	81.10(5)	S(1)–Mo(1)–S(2)	108.54(6)
S(1)–Mo(1)–S(4)	107.29(5)	S(2)–Mo(1)–S(4)	87.35(5)
S(1)–Mo(2)–S(2)	108.45(6)	S(1)–Mo(2)–S(3)	109.65(5)
S(2)–Mo(2)–S(3)	86.16(5)	S(1)–Mo(3)–S(3)	109.51(5)
S(1)–Mo(3)–S(4)	107.16(5)	S(3)–Mo(3)–S(4)	86.21(5)
O(1)–Mo(1)–O(2)	77.41(18)	O(1)–Mo(1)–O(3)	78.7(2)
O(2)–Mo(1)–O(3)	81.16(18)	O(4)–Mo(2)–O(5)	77.66(16)
O(4)–Mo(2)–O(2)	80.39(16)	O(5)–Mo(2)–O(6)	83.29(16)
O(7)–Mo(3)–O(8)	78.99(17)	O(7)–Mo(3)–O(9)	76.02(16)
O(8)–Mo(3)–O(9)	80.81(16)	Mo(1)–S(1)–Mo(2)	70.80(4)
Mo(1)–S(1)–Mo(3)	71.95(4)	Mo(2)–S(1)–Mo(3)	70.04(4)
Mo(1)–S(2)–Mo(2)	70.97(5)	Mo(1)–S(2)–As(1)	94.71(5)
Mo(2)–S(2)–As(1)	96.70(5)	Mo(2)–S(3)–Mo(3)	70.05(4)
Mo(2)–S(3)–As(1)	95.42(5)	Mo(3)–S(3)–As(1)	95.22(5)
Mo(1)–S(4)–Mo(3)	71.98(4)	Mo(1)–S(4)–As(1)	94.92(5)
Mo(3)–S(4)–As(1)	96.79(5)		

Table 3. UV–vis Absorbance Spectra of $[\text{Mo}_3\text{S}_4(\text{H}_2\text{O})_9]^{4+}$ and $[\text{Mo}_6\text{AsS}_8(\text{H}_2\text{O})_{18}]^{8+}$ in both 2.0 M HCl and 2.0 M H(pts)^a

cluster	acid	λ ($10^{-3}\epsilon$)
$[\text{Mo}_3\text{S}_4(\text{H}_2\text{O})_9]^{4+}$	2.0 M HCl	370 (5.0), 616 (0.33)
	2.0 M H(pts)	366 (5.5), 603 (0.36)
$[\text{Mo}_6\text{AsS}_8(\text{H}_2\text{O})_{18}]^{8+}$	2.0 M HCl	391 (12.1), 609 (9.8)
	2.0 M H(pts)	379 (12.7), 595 (9.7)

^a Peak positions (λ/nm) and absorption coefficients ($\epsilon/\text{M}^{-1}\text{cm}^{-1}$) per Mo_3 or Mo_6 are indicated.

as expected in view of the significant Mo–Mo bonding interactions (mean 2.716 Å) and lack of direct Mo–As bonding (mean 3.554 Å).

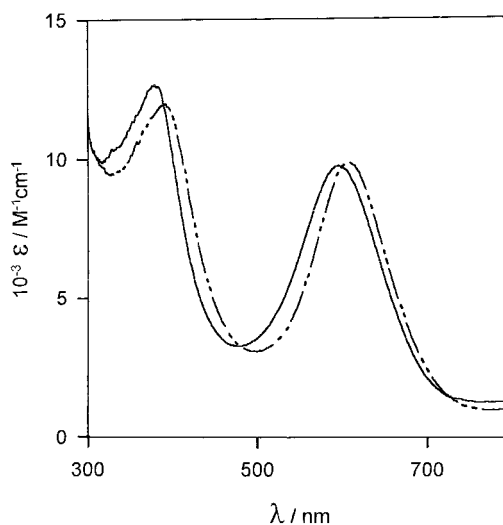
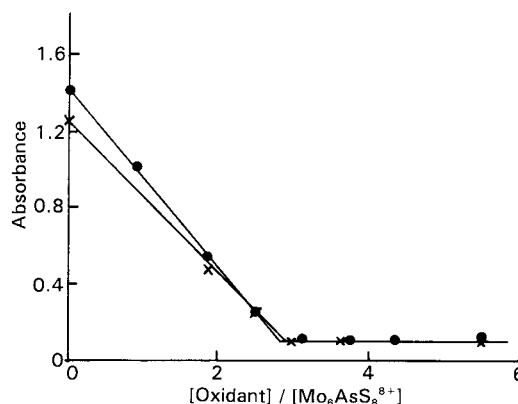
Aqua ligands, pts[−] anions, and molecules of water of crystallization are held together by a complex network of hydrogen bonding, which is not sufficiently strong to prevent disorder in the anions and water molecules, but the key element of the structure, the double-cube cation, is well ordered.

UV–Vis Spectrum. Details of peak positions and absorption coefficients (ϵ) in 2.0 M HCl and 2.0 M H(pts) are given in Table 3. The ϵ values were determined by allowing a solution of $[\text{Mo}_6\text{AsS}_8(\text{H}_2\text{O})_{18}]^{8+}$ to oxidize in air. The only Mo-containing product is the incomplete cube $[\text{Mo}_3\text{S}_4(\text{H}_2\text{O})_9]^{4+}$,



the UV–vis spectrum of which is known in the same two acids, Table 3. Some oxidation of As^{III} to As^V will also occur. The two spectra, Figure 2, are very similar, with differences most likely due to Cl[−] complexing to Mo.

Stability of $[\text{Mo}_6\text{AsS}_8(\text{H}_2\text{O})_{18}]^{8+}$. The cluster is very air-sensitive, and rigorous air-free conditions are required at all times. The cluster is more stable to air oxidation in HCl than in H(pts) solutions. In 2.0 M HCl there is a 25% decay in 1 h, while in H(pts) there is 79% decay in 30 min (solutions were contained in an optical cell with some shaking). This relatively small change is opposite to that observed for the group 13 heteroatom double cubes and, in particular $[\text{Mo}_6\text{TlS}_8(\text{H}_2\text{O})_{18}]^{8+}$,

**Figure 2.** UV–vis spectra of $[\text{Mo}_6\text{AsS}_8(\text{H}_2\text{O})_{18}]^{8+}$ (ϵ 's per Mo_6) in 2.0 M acids, H(pts) (—) and HCl (---).**Figure 3.** Determination of the stoichiometry for the oxidation of $[\text{Mo}_6\text{AsS}_8(\text{H}_2\text{O})_{18}]^{8+}$ (1.2×10^{-4} M): (A) by $[\text{Co}(\text{dipic})_2]^-$ (2.0 mM, ●) and (B) by $[\text{Fe}(\text{H}_2\text{O})_6]^{3+}$ (1.88 mM, ×) in 2.0 M H(pts). The procedure involved titrating in the oxidant from a microsyringe and monitoring absorbance changes of the solution in an optical cell (1×1 cm² cross section, volume ~ 3 mL) at 595 nm.

which is much more stable in H(pts) solutions.^{10,11} No evidence was obtained for products other than the 8+ double cube in the chromatography, and in redox studies no evidence was obtained for intermediate formation of a single cube with core composition $\text{Mo}_3\text{AsS}_4^{7+}$, which, in view of the high charge density, is likely to be short-lived. An air-free 2 M H(pts) solution of the cluster in an optical cell, concentration ~ 0.1 mM, gave only $\sim 3\%$ decay in 30 min, representing maximum instability of the double cube. Solutions of $[\text{Mo}_6\text{AsS}_8(\text{H}_2\text{O})_{18}]^{8+}$ were stable with $[\text{H}^+]$ as low as 0.10 M. No oxidation was observed on addition of HClO_4 to 1.0 M.

Stoichiometry of Oxidation. Solutions of $[\text{Mo}_6\text{AsS}_8(\text{H}_2\text{O})_{18}]^{8+}$ (~ 0.12 mM) in 2.0 M H(pts) contained in an optical cell were titrated with more concentrated solutions of the oxidants $[\text{Co}(\text{dipic})_2]^-$ and $[\text{Fe}(\text{H}_2\text{O})_6]^{3+}$ from a 0.25-mL Hamilton microsyringe. In both cases, oxidation was rapid (1 min required after addition of each aliquot), and absorbance changes at 595 nm were monitored, Figure 3. Rigorous air-free (N_2) conditions were required. Exploratory experiments were carried out to determine approximate stoichiometries prior to those illustrated in Figure 3, when fewer points were included for the earlier part of the titration so as to gain better precision at the end point. There was no evidence for buildup of any intermediate form. The sole Mo-containing product was

$[\text{Mo}_3\text{S}_4(\text{H}_2\text{O})_9]^{4+}$, with peaks in the UV–vis spectrum 366–(5550) and 603(362) in 2.0 M H(pts).⁵ Stoichiometries of 1:2.85 with $[\text{Co}(\text{dipic})_2]^-$ and 1:2.90 with $[\text{Fe}(\text{H}_2\text{O})_6]^{3+}$ are consistent with (5) and (6).



The equations require the double cube to be present as an 8+ ion to give the products indicated. Reduction potentials for the oxidants are $[\text{Co}(\text{dipic})_2]^{-/2-}$, 362 mV, and $[\text{Fe}(\text{H}_2\text{O})_6]^{3+/2+}$, 770 mV. The first of these is a revised value recently determined²⁴ and should be used in place of a previously quoted literature value. The stoichiometry observed in (6) implies that the Fe^{III} oxidation of As^{III} does not contribute to the reaction as carried out and is a relatively slow process.

Kinetics of the Oxidation with $[\text{Co}(\text{dipic})_2]^-$. The oxidation of $[\text{Mo}_6\text{AsS}_8(\text{H}_2\text{O})_{18}]^{8+}$ by $[\text{Co}(\text{dipic})_2]^-$ was monitored by stopped-flow spectrophotometry at the 595-nm peak of the double cube. First-order rate constants k_{obs} (25 °C) were determined for the uniphasic decay process with $[\text{Co}(\text{dipic})_2]^-$ in ≥ 30 -fold excess over $[\text{Mo}_6\text{AsS}_8(\text{H}_2\text{O})_{18}]^{8+}$ (see listing in Supporting Information). A linear dependence of k_{obs} on $[\text{Co}(\text{dipic})_2]^-$ is observed, Figure 4, consistent with the rate law (7).



No $[\text{H}^+]$ dependence was observed in the $[\text{H}^+]$ range 0.5–2.0 M, $I = 2.00$ M (Li(pts)). From the slope using an unweighted least-squares treatment $k_{\text{Co}} = 21.0 (\pm 0.1) \times 10^3 \text{ M}^{-1} \text{ s}^{-1}$. Since uniphasic changes are observed with no evidence for buildup of an intermediate, the following reaction sequence involving transient formation of a 9+ double cube is proposed:



The rate constant k_{Co} is toward the high end of the range of values determined for the oxidation of different double cubes with $[\text{Co}(\text{dipic})_2]^-$, Table 5.

The oxidation of $[\text{Mo}_6\text{AsS}_8(\text{H}_2\text{O})_{18}]^{8+}$ in 2.0 M HCl was also studied briefly when the reaction was found to be ~ 200 times slower than that in 2.0 M H(pts).

Discussion

The preparation and characterization of $[\text{Mo}_6\text{AsS}_8(\text{H}_2\text{O})_{18}]^{8+}$ establishes arsenic as a further example of a main group element forming a corner-shared double-cube derivative of $[\text{Mo}_3\text{S}_4(\text{H}_2\text{O})_9]^{4+}$. The product is of particular interest because arsenic is not generally regarded as a metallic element alongside the heavier group 15 metals and is the first nonmetallic element to be incorporated in this way. ICP elemental analyses, cation-exchange properties, and redox stoichiometries alongside the X-ray crystal structure determination provide confirmation of the corner-shared double-cube structure.

Three group 15 elements, As, Sb, and Bi, have now been incorporated into corner-shared double cubes $[\text{Mo}_6\text{MS}_8(\text{H}_2\text{O})_{18}]^{8+}$. In Table 4, UV–vis peak positions (charge-transfer

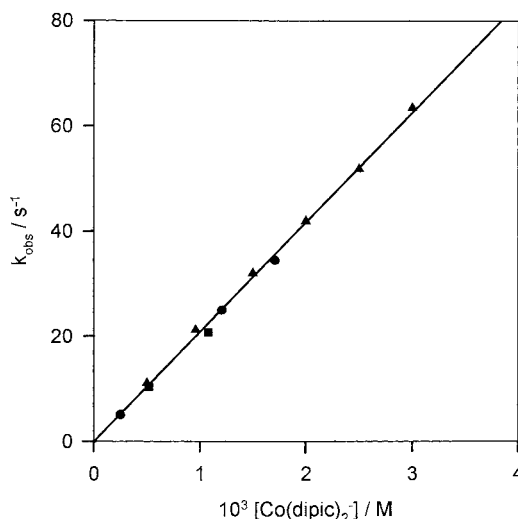


Figure 4. Dependence of first-order rate constants k_{obs} (25 °C) for the $[\text{Co}(\text{dipic})_2]^-$ (reactant in large excess) oxidation of $[\text{Mo}_6\text{AsS}_8(\text{H}_2\text{O})_{18}]^{8+}$ on concentration of oxidant. No dependence on $[\text{H}^+] = 2.0$ (\blacktriangle), 1.0 (\bullet), and 0.50 (\blacksquare) is observed, $I = 2.0$ M (Li(pts)).

Table 4. Summary of UV–vis Peak Positions (λ/nm ($\epsilon/\text{M}^{-1}\text{cm}^{-1}$ per Mo_6)) for Corner-Shared Double Cubes $[\text{Mo}_6\text{MS}_8(\text{H}_2\text{O})_{18}]^{8+}$ in 2.0 M H(pts)

M	λ ($10^{-3} \epsilon$)	ref
As	379 (12.7), 595 (9.7)	this work
Sb	385 (6.1), ^a 620 (4.0) ^a	4
Bi	366 (9.3), 586 (3.12)	5
Sn	379 (22.1), 544 (15.5)	6, 7
Pb	392 (14.6), 757 (2.73)	8
In	379 (21.8), 486 (6.65)	10
Tl	380 (12.9), 660 (14.2)	11
Hg	372 (13.0), 556 (18.8)	12

^a It is not clear whether ϵ 's quoted are per molecule.

Table 5. Summary of Rate Constants (25 °C) for the Oxidation of Corner-Shared Double-Cube Clusters $[\text{Mo}_6\text{MS}_8(\text{H}_2\text{O})_{18}]^{8+}$ with $[\text{Co}(\text{dipic})_2]^-$ in Aqueous H(pts) Solutions^a

M	$k_{\text{Co}}/\text{M}^{-1} \text{ s}^{-1}$	ref
As	2.10×10^4	this work
Bi	3.6×10^4	5
Sn	14.9	7
Pb	2.76×10^5	8
In	3.09×10^4	10
Mo	0.31	20

^a $I = 2.00$ M (Li(pts)).

transitions) are listed. A narrow spread of peak positions is observed in the case of M = As (blue-green), Bi (turquoise-blue), Sb (blue-green), Tl (turquoise), and Pb (blue-green). There are some similarities with the spectrum of $[\text{Mo}_3\text{S}_4(\text{H}_2\text{O})_9]^{4+}$, Table 3. Other clusters with M = Sn (red-purple), Hg (purple), and In (red-brown) have the second peak shifted to lower wavelengths, while $[\text{Mo}_7\text{S}_8(\text{H}_2\text{O})_{18}]^{8+}$ (violet), with peaks at 416, 480(sh), 518, and 635 nm, has a different, more detailed spectrum.²⁰

Rate constants (25 °C, $\text{M}^{-1} \text{ s}^{-1}$) for outer-sphere oxidation with $[\text{Co}(\text{dipic})_2]^-$ in 2.0 M H(pts) (independent of $[\text{H}^+]$) have been determined, Table 5. In the case of the group 15 heteroatoms, the values obtained for M = As (2.1×10^4) and Bi (3.6×10^4) are, surprisingly, very similar. Both the As and Bi double cubes are toward the high end of reactivities observed for the double cube but are more midrange ($1\text{--}10^6 \text{ M}^{-1} \text{ s}^{-1}$) with the inclusion of the single cubes.²⁵ Such rate constants also provide a guide as to the sensitivity of reaction

(24) Saysell, C. G.; Borman, C. D.; Baron, A. J.; McPherson, M. J.; Sykes, A. G. *Inorg. Chem.* **1997**, *36*, 4520.

Table 6. X-ray Crystallographic Information for Aqua Ions (Except As Indicated) of Double- and Single-Cube Heteroatom Derivatives of $[\text{Mo}_3\text{S}_4(\text{H}_2\text{O})_9]^{4+}$

	Mo–Mo (Å)	Mo–M (Å)	ref
Double Cubes			
$\text{Mo}_7\text{S}_8^{8+}$ ^a	2.770	3.046 ^a	26
$\text{Mo}_6\text{HgS}_8^{8+}$	2.713	3.830	12
$\text{Mo}_6\text{InS}_8\text{O}_2^{8+}$	2.627	3.583	9
$\text{Mo}_6\text{SnS}_8^{8+}$	2.688	3.713	6
$\text{Mo}_6\text{AsS}_8^{8+}$	2.716	3.554	this work
Single Cubes			
$\text{Mo}_3\text{S}_4^{4+}$ ^b	2.732		33
$\text{Mo}_3\text{GaS}_4^{5+}$	2.713	3.520	34
$\text{Mo}_3\text{InS}_4^{5+}$	2.682	3.720	35
$\text{Mo}_3\text{SnS}_4^{6+}$ ^c	2.730	3.732	7
$\text{Mo}_3\text{PbS}_4^{6+}$ ^d	2.747	4.207	36
$\text{Mo}_3\text{BiS}_4^{7+}$ ^d	2.732	4.132	36
$\text{Mo}_3\text{FeS}_4^{4+}$ ^e	2.793	2.683	38
$\{\text{Mo}_3\text{CoS}_4^{4+}\}_2$ ^f	2.744	2.643	39
$\text{Mo}_3\text{NiS}_4^{4+}$	2.744	2.678	40
$\{\text{Mo}_3\text{CuS}_4^{4+}\}_2$ ^f	2.730	2.887	41
$\text{Mo}_3\text{PdS}_4^{4+}$ ^g	2.819	2.793	42
$\{\text{Mo}_3\text{PdS}_4\}_2$ ^f	2.773	2.799	42
$\text{Mo}_4\text{S}_4^{5+}$	2.802		45
$\text{Mo}_4\text{S}_4^{4+}$ ^e	2.797		46

^a M is nodal Mo. ^b Incomplete cube. ^c NCS^- and Cl^- ligands. ^d dtp ligands. ^e NH_3 ligands. ^f Edge linked double cube. ^g tacn ligands.

with O_2 , which virtually all the heteroatom derivatives of $[\text{Mo}_3\text{S}_4(\text{H}_2\text{O})_9]^{4+}$ exhibit, and, more generally, are a mark of redox properties, since the determination of reduction potentials by CV electrochemical methods has proved difficult.

The list of corner-shared double cubes now includes group 12 (Hg),¹² group 13 (In, Tl),^{9–11} group 14 (Sn, Pb),^{6–8} and group 15 (As, Sb, Bi) elements.^{4,5} X-ray crystal structures have been reported for the Hg-¹² In- (as an $\text{Mo}_3\text{OS}_3^{4+}$ derivative),⁹ Sn-⁶ As-, and Sb-containing clusters. The only example of a corner-shared double cube with a transition metal at the nodal position is $[\text{Mo}_7\text{S}_8(\text{H}_2\text{O})_{18}]^{8+}$.²⁶ An unusual feature is that all nine double cubes have an 8+ charge.

We have previously made the point²⁰ that X-ray crystal structure information for single and double cubes provides evidence for Mo–Mo metal–metal bonding. Short Mo–M separations are observed when M is a transition metal, but not when M is a main group element, Table 6. A further example is provided by $[\text{Mo}_6\text{AsS}_8(\text{H}_2\text{O})_{18}]^{8+}$, which has short Mo–Mo distances averaging 2.716 Å, whereas the six Mo–As distances averaging 3.554 Å indicate a nonbonding situation. The As–S distances are also long. Theoretical attempts to better understand cuboidal clusters have ranged from qualitative and approximate molecular orbital treatment^{27–29} to more exact spin and space unrestricted X_α calculations.^{30,31} Harris has considered different classes of heterometallic clusters $\text{M}_3\text{M}'\text{S}_4$ based on different metal coordination geometries and a situation in which stronger metal/ligand interactions are accompanied by weaker metal–metal

interactions.³² However, the latter review preceded the identification of main group heteroatoms which are now known to have a significant role in this chemistry. The proposals which we make are able to account for the 8+ charge of the corner-shared double cubes and other features. Many of the Mo–Mo distances in Table 6 are similar to the 2.732 Å average value reported for $[\text{Mo}_3\text{S}_4(\text{H}_2\text{O})_9](\text{pts})_4 \cdot 9\text{H}_2\text{O}$,³³ which is diamagnetic and has a triangular arrangement of three metal–metal bonded Mo^{IV} (d^2) centers. The $[\text{Mo}_6\text{MS}_8(\text{H}_2\text{O})_{18}]^{8+}$ cubes are considered first, where M is generally a main group element from groups 12–15. The constant 8+ overall charge suggests that two $\text{Mo}_3\text{S}_4^{4+}$ units are retained and are a common feature. These are bridged by an M^0 atom. The Mo–M separations are ~ 1 Å longer than for Mo–Mo, and no Mo–M metal–metal bonding is apparent, Table 6. Consistent with this approach, the mercury-containing double cube $[\text{Mo}_6\text{HgS}_8(\text{H}_2\text{O})_{18}]^{8+}$ was assigned as Hg^0 on the basis of Hg–S bond lengths at the time the crystal structure was reported.¹² Formulas of the double cubes can, therefore, be written as $(\text{Mo}_3\text{S}_4^{4+})_2\text{M}^0$. There are also three X-ray crystal structures of single cubes with main group heteroatoms M, namely $[\text{Mo}_3\text{MS}_4(\text{H}_2\text{O})_{12}]^{5+}$ ($\text{M} = \text{Ga}, \text{In}$)^{34,35} and $[\text{Mo}_3\text{MS}_4(\text{H}_2\text{O})_{12}]^{6+}$ ($\text{M} = \text{Sn}$).⁷ Here, the cores are written as $\text{Mo}_3\text{S}_4^{4+}\text{M}^+$ ($\text{M} = \text{In}, \text{Ga}$) and $\text{Mo}_3\text{S}_4^{4+}\text{M}^{2+}$ ($\text{M} = \text{Sn}$), consistent with the 5+ and 6+ structures already indicated. In recent Fuzhuo work,³⁶ $[\text{Mo}_3(\text{PbI}_3)\text{S}_4(\text{dtp})_3(\text{py})_3]$ and $[\text{Mo}_3(\text{BiI}_3)\text{S}_4(\text{dtp})_3(\mu\text{O}_2\text{CMe})(\text{py})]$ ($\text{dtp} = \text{S}_2\text{P}(\text{OC}_2\text{H}_5)_2^-$; $\text{py} = \text{pyridine}$) clusters containing $\text{Mo}_3\text{PbS}_4^{6+}$ and $\text{Mo}_3\text{BiS}_4^{7+}$ cores, respectively, have been isolated for the first time; these can alternatively be written as $\text{Mo}_3\text{S}_4^{4+}\text{Pb}^{2+}$ and $\text{Mo}_3\text{S}_4^{4+}\text{Bi}^{3+}$. In the latter cases, the negatively charged ligands help balance the high charge on the core with stabilization of the single cube. Finally, when M is a transition metal (e.g., Cr, Fe, Co, Ni, Cu, or Pd),^{37–42} single cubes of 4+ charge are obtained, and the heteroatom M can, at least in some cases, be designated as M^0 . The short Mo–M bond lengths from crystallography provide evidence for Mo–M bonding in these cubes.

With the corner-shared double cube $[\text{Mo}_7\text{S}_8(\text{H}_2\text{O})_{18}]^{8+}$, the only example at present which has a transition metal at the nodal position, each cube has three short (2.770 Å) and three long (3.046 Å) Mo–Mo (nodal) separations.²⁰ Here it would appear the central Mo has less strong Mo–Mo bonding. A structure approximating to $(\text{Mo}_3\text{S}_4^{4+})_2\text{Mo}^0$ with adjacent Mo' assigned as Mo^{IV} and Mo^0 is clearly less satisfactory, and some sort of intermediate oxidation state assignment may be appropriate. This could also account for the different type of UV–vis spectrum.

The arsenic-containing double cube $[\text{Mo}_6\text{AsS}_8(\text{H}_2\text{O})_{18}]^{8+}$ has only the one stable oxidation state in keeping with other

- (25) Dimmock, P. W.; Saysell, D. M.; Sykes, A. G. *Inorg. Chim. Acta* **1994**, *225*, 157.
 (26) Shibahara, T.; Yamamoto, T.; Kanadani, H.; Kuroya, H. *J. Am. Chem. Soc.* **1987**, *109*, 3495.
 (27) Chu, C. T.-W.; Lo, F. Y.-K.; Dahl, L. F. *J. Am. Chem. Soc.* **1982**, *104*, 3409.
 (28) Müller, A.; Joster, R.; Eltner, W.; Nie, C.-S.; Diemann, E.; Bögge, H.; Zimmerman, M.; Dartmann, M.; Reinsch-Vogell, U.; Che, S.; Cyvin, S. J.; Cyvin, B. N. *Inorg. Chem.* **1985**, *24*, 2872.
 (29) Williams, P. D.; Curtis, M. D. *Inorg. Chem.* **1986**, *25*, 4562.
 (30) Noodleman, L.; Norman, J. C., Jr.; Osborne, J. H.; Aizman, A.; Case, D. A. *J. Am. Chem. Soc.* **1985**, *107*, 3418.
 (31) Darkwa, J.; Lockemeyer, J. R.; Boyd, P. D. W.; Rauchfuss, J. B.; Rheingold, A. L. *J. Am. Chem. Soc.* **1988**, *110*, 141.

- (32) Harris, S. *Polyhedron* **1989**, *8*, 2843–2882.
 (33) Akashi, H.; Shibahara, T.; Kuroya, H. *Polyhedron* **1990**, *9*, 1671.
 (34) Shibahara, T.; Kobayashi, S.; Tsuji, N.; Sakane, G.; Fukuhara, M. *Inorg. Chem.* **1997**, *36*, 1702.
 (35) Sakane, G.; Shibahara, T. *Inorg. Chem.* **1993**, *32*, 777.
 (36) Lu, S. F.; Huang, J.-Q.; Wu, Q.-J.; Huang, X.-Y.; Yu, R.-M.; Zheng, Y.; Wu, D.-X. *Inorg. Chim. Acta* **1997**, *261*, 201.
 (37) Routledge, C. A.; Humanes, M.; Li, Y.-J.; Sykes, A. G. *J. Chem. Soc., Dalton Trans.* **1994**, 1275.
 (38) Shibahara, T.; Akashi, H.; Kuroya, H. *J. Am. Chem. Soc.* **1986**, *108*, 1342.
 (39) (a) Shibahara, T.; Akashi, H.; Yamasaki, M.; Hashimoto, K. *Chem. Lett.* **1991**, 689. (b) Dimmock, P. W.; Saysell, D. M.; Sykes, A. G. *Inorg. Chim. Acta* **1994**, *225*, 157.
 (40) Shibahara, T.; Yamasaki, M.; Akashi, H.; Katayama, T. *Inorg. Chem.* **1991**, *30*, 2693.
 (41) Shibahara, T.; Akashi, H.; Kuroya, H. *J. Am. Chem. Soc.* **1988**, *110*, 3313.
 (42) Murata, T.; Mizobe, Y.; Gao, H.; Ishii, Y.; Wakabayashi, T.; Nakono, F.; Tarase, T.; Yano, S.; Hidai, M.; Echizen, J.; Nanikawa, H.; Motomura, S. *J. Am. Chem. Soc.* **1994**, *116*, 3389.

heteroatom single and double cubes ($M = \text{Cu}$ is the only exception⁴³). The $[\text{Mo}_4\text{S}_4(\text{H}_2\text{O})_{12}]^{n+}$ cubes are a special case in that three oxidation states, $n = 4, 5,$ and $6,$ have been isolated. Of these, the Mo^{III}_4 cluster $[\text{Mo}_4\text{S}_4(\text{H}_2\text{O})_{12}]^{4+}$ has $12e^-$, sufficient for the maximum number (six) of Mo–Mo bonds. Because of its air sensitivity, the latter is often regarded as less stable than $[\text{Mo}_4\text{S}_4(\text{H}_2\text{O})_{12}]^{5+}$, which has only $11e^-$. However both the $5+$ and $6+$ clusters have tendencies to fragment in air. For the $5+$ cube, a high temperature of $\sim 90^\circ\text{C}$ is required,¹⁹ but for the $6+$ cube decay is complete in ~ 40 h at 25°C .⁴⁴ This instability could, to some extent, reflect the high charge density as well as the electron deficiencies. The Mo–Mo bond lengths for the $4+$ and $5+$ cubes are included in Table 6. The difficulties so far experienced in preparing vanadium and titanium derivatives of $[\text{Mo}_3\text{S}_4(\text{H}_2\text{O})_9]^{4+}$ ²⁰ most likely relate to the low d electron populations of these elements.

(43) Nasreldin, M.; Li, Y.-J.; Mabbs, F. E.; Sykes, A. G. *Inorg. Chem.* **1994**, *33*, 4283.

(44) Hong, M.-C.; Li, Y.-J.; Lu, J.-X.; Nasreldin, M.; Sykes, A. G. *J. Chem. Soc. Dalton Trans.* **1993**, 2613.

(45) Akashi, H.; Shibahara, T.; Narahara, T.; Tsuru, H.; Kuroya, H. *Chem. Lett.* **1989**, 129.

(46) Shibahara, T.; Kawano, E.; Okano, M.; Nishi, M.; Kuroya, H. *Chem. Lett.* **1986**, 827.

To summarize, the isolation and characterization of the corner-shared double cube $[\text{Mo}_6\text{AsS}_8(\text{H}_2\text{O})_{18}]^{8+}$ is of considerable interest, first because of the largely nonmetallic properties of arsenic. We note also that there are now nine such double cubes $[\text{Mo}_6\text{MS}_8(\text{H}_2\text{O})_{18}]^{8+}$ ($M = \text{Hg}, \text{In}, \text{Tl}, \text{Sn}, \text{Pb}, \text{As}, \text{Sb}, \text{Bi},$ and Mo), all of which have an $8+$ charge. Metal–metal bonding is extremely important in considering the different categories of cube, and structures can be rationalized by retention of the $\text{Mo}_3\text{S}_4^{4+}$ unit. The formalism adopted, although ignoring interactions between the heteroatoms and core sulfides, is able to account for all aqua (and other complexes) so far isolated as derivatives of $[\text{Mo}_3\text{S}_4(\text{H}_2\text{O})_9]^{4+}$.

Acknowledgment. We thank the European Union for HEMP network grant ERBCHRX-CT94-0632 in support of this work and the University of La Laguna in Tenerife for a leave of absence (R.H.-M). We are also grateful to the UK Engineering Physical Sciences Research Council for an equipment grant.

Supporting Information Available: Listing of rate constants (1 page). One X-ray crystallographic file, in CIF format, is available on the Internet only. Ordering and access information is given on any current masthead page.

IC971570B